Hamiltonian studies of the Blume-Emery-Griffiths model

F. C. Alcaraz
Departamento de Física, Universidade Federal de São Carlos, Caixa Postal 616, CEP-13560 São Carlos, São Paulo, Brazil

J. R. Drugowich de Felício and R. Köberle
Departamento de Física e Ciência dos Materiais, Instituto de Física e Química de São Carlos, Universidade de São Paulo, Caixa Postal 369, CEP-13560 São Carlos, São Paulo, Brazil

J. F. Stilck*
Instituto de Física, Universidade de São Paulo, Caixa Postal 20516, CEP-01498 São Paulo, São Paulo, Brazil
(Received 17 December 1984; revised manuscript received 4 June 1985)

Finite-size scaling methods are used to obtain the phase diagram of the Blume-Emery-Griffiths model in its time-continuous Hamiltonian version. In particular, we locate the tricritical point, where a first-order transition changes to one of second order, and evaluate its exponents. The exponents are in complete agreement with Nienhuis' conjecture. We also discuss a recent conjecture concerning the universality of the ratio of mass-gap amplitudes. Our results suggest the validity of this conjecture even at the tricritical point.

I. INTRODUCTION

The Blume-Emery-Griffiths[1] (BEG) model is a spin-1 model which has been used to describe the behavior of ^{3}He-^{4}He mixtures along the λ line and near the critical mixing point. Apart from its practical interest (it reproduces at least qualitatively the main features of the phase diagram for superfluid and phase-separation transitions), the BEG model has intrinsic interest since it is the simplest generalization of the spin-$\frac{1}{2}$ Ising model[2] exhibiting a complex phase diagram with first- and second-order transition lines and tricritical points. The predictions of the conventional mean-field theory are essentially correct for $d\,(d \geq 3)$ dimensional models. However, they are even qualitatively incorrect for the two-dimensional (2D) lattice. The failure of the mean-field approximation has led to several studies of the 2D classical BEG model, such as the renormalization-group,[3] ϵ expansion[4] downwards from $d=3$, Migdal-Kadanoff renormalization scheme,[5] and Monte Carlo renormalization-group[6] approximations.

This model can also be mapped, in the usual fashion, into a one-dimensional quantum model[7] which is believed to share the same critical behavior with its classical counterpart. In its quantum version, the BEG model has been analyzed by real-space renormalization group[7,8] and mean-field-like variational methods.[7]

The purpose of this paper is to obtain the phase diagram and critical properties of the BEG model in its quantum version, using the finite-size scaling[9] (FSS) approach. The motivation is the recent success of the FSS, in transfer-matrix calculations,[10] in obtaining a tricritical point and its leading exponents.

Our paper is organized as follows. In Sec. II we present the model as well as its quantum version. Section III contains a brief introduction to finite-size ideas and their extension to the study of tricritical behavior. The critical point is obtained with high precision, and the critical exponents are evaluated by using two different methods. Finally, in Sec. IV we calculate the mass-gap amplitudes at the tricritical point. Our results corroborate the recent conjecture concerning the universality of mass-gap amplitude ratios.

II. MODEL

We consider a spin variable $S(i,j)$ which assumes values 1, 0, or -1, associated with each site of a square lattice. The BEG dynamics is described by the Hamiltonian

$$\begin{aligned}\mathscr{H}=&-J_x\sum_{i,j}S(i,j)S(i+1,j)\\&-K_x\sum_{i,j}S^2(i,j)S^2(i+1,j)-J_t\sum_{i,j}S(i,j)S(i,j+1)\\&-K_t\sum_{i,j}S^2(i,j)S^2(i,j+1)+\Delta\sum_{i,j}S^2(i,j)\ ,\end{aligned}\tag{1}$$

where Δ is a single-state energy, J_x and K_x (J_t and K_t), are, respectively, exchange and quadrupolelike interactions in the horizontal (vertical) direction.

The transfer matrix associated with this model, with periodic boundary conditions in the t direction, can be obtained by a standard procedure[7] and it is given by

$$T=e^{-H_1/2}e^{-H_0}e^{-H_1/2}\ ,\tag{2}$$

where

$$H_0=X\sum_i S_x(i)+Z\sum_i S_x^2(i)\ ,\tag{3a}$$

$$\begin{aligned}H_1=&Y\sum_i S_Z^2(i)-\beta J_x\sum_i S_z(i)S_z(i+1)\\&-\beta K_x\sum_i S_z^2(i)S_z^2(i+1)\ ,\end{aligned}\tag{3b}$$

and $S_x(i), S_z(i)$ are now quantum spin-1 operators represented by

$$S_\omega = \mathbb{1}\otimes\mathbb{1}\otimes\cdots\otimes\hat{S}_\omega\otimes\cdots\otimes\mathbb{1}\ ,\quad \omega=x,z\ ,$$

with

$$\hat{S}_x=\frac{1}{\sqrt{2}}\begin{bmatrix}0&1&0\\1&0&1\\0&1&0\end{bmatrix}\ ,\quad \hat{S}_z=\begin{bmatrix}1&0&0\\0&0&0\\0&0&-1\end{bmatrix} \tag{4}$$

acting on the product Hilbert space.

The new coupling X, Y, and Z appearing in Eq. (3) can be written in terms of the original couplings as follows:

$$\sinh^2 X = e^{-\beta K_t}[\cosh(\beta J_t)-e^{-\beta K_t}]^{-1}\ , \tag{5a}$$

$$e^{-2Z}=\frac{\cosh(\beta J_t)}{\sinh^2(\beta J_t)}[\cosh(\beta J_t)-e^{-\beta K_t}]\ , \tag{5b}$$

$$Y=\beta\Delta-\ln[2e^{+\beta K_t}\cosh(\beta J_t)]\ . \tag{5c}$$

The transfer matrix T commutes with the parity operator

$$\mathscr{P}=\prod_i \otimes[\hat{S}_x^2(i)-\mathbb{1}]\ , \tag{6a}$$

$$\mathscr{P}^2=\mathbb{1}\otimes\cdots\otimes\mathbb{1}\ . \tag{6b}$$

It is this $Z(2)$ invariance of T which will be spontaneously broken along the transition line.

We want to stress that the transfer matrix has almost all elements nonzero, because it is formed by a product of operators. Consequently, it is difficult to compute its spectrum, even for relatively small lattices. To circumvent this problem we will derive an equivalent quantum Hamiltonian (which is a sum of operators) which is expected to preserve the long-distance behavior, and whose spectrum determination is an easier task.

In order to get this equivalent Hamiltonian we need to consider a highly anisotropic limit in which X, Y, Z, J_x, and K_x are very small numbers. This limit is achieved by choosing

$$\beta J_x, \beta K_x \ll 1\ , \tag{7a}$$

and simultaneously

$$\beta J_t, \beta K_t \gg 1\ , \tag{7b}$$

under the restriction

$$\beta(\Delta - J_t - K_t) \ll 1\ . \tag{7c}$$

The quantum Hamiltonian so obtained is

$$H=-\sum_i [S_z(i)S_z(i+1)-\alpha S_z^2(i)S_z^2(i+1) -\delta S_z^2(i)-\gamma S_x(i)-\lambda S_x^2(i)]\ , \tag{8a}$$

with

$$\alpha=\frac{K_x}{J_x}\ ,\quad \delta=\frac{Y}{\beta J_x}\ ,\quad \gamma=\frac{X}{\beta J_x}\ ,\quad \lambda=\frac{Z}{\beta J_x}\ . \tag{8b}$$

III. FINITE-SIZE SCALING

In this section we shall present the finite-size scaling method used to obtain the phase diagram (including the tricritical point) of the quantum Hamiltonian [Eq. (8)] associated with the 2D classical BEG model.

The FSS method had its genesis in the works of Fisher, Ferdinand, and Barber[11] in which the finite-size effects on criticality were studied. Later, Nightingale[9] introduced a phenomenological renormalization group,[12] which permits one to obtain the true infinite critical behavior from the analysis of small systems. An appropriate form of the FSS can also be stated for a quantum Hamiltonian.[13] The fundamental assumption of the FSS theory, in this case, is that the mass gap G (related to the correlation length), which is an infinite system, varies near a critical coupling β_c as

$$G(\beta)=(E_1-E_0)\sim(\beta-\beta_c)^\nu\ , \tag{9a}$$

and for a finite system of size L, behaves as

$$G_L(\beta_c)\sim L^{-1}\ . \tag{9b}$$

In Eq. (9a), E_0 (E_1) is the energy of the ground (first-excited) state of the Hamiltonian H.

The FSS form suggests that β_c can be found from the sequence of values β for which the successive ratios of $G_L(\beta)$ and $G_{L-1}(\beta)$ exactly scale, i.e., the value of β for which[14]

$$R_L = LG_L(\beta)/(L-1)G_{L-1}(\beta)\ . \tag{10}$$

In general, any thermodynamical quantity $Q(\beta)$ whose infinite lattice behavior is

$$Q(\beta)\sim(\beta-\beta_c)^{-\psi}\ , \tag{11}$$

in the finite system scales as

$$Q_L(\beta_c)\sim L^{\psi/\nu}\ . \tag{12}$$

Therefore, by considering a set of finite lattices it is possible to estimate the index ψ/ν by extrapolating the sequence

$$\{L[Q_L(\beta_c)-Q_{L-1}(\beta_c)]/Q_{L-1}(\beta_c)\}\rightarrow\psi/\nu\ . \tag{13}$$

In particular, to obtain the critical exponent ν the extrapolation should be done with

$$Q_L(\beta)=\frac{1}{G_L(\beta)}\frac{\partial G_L(\beta)}{\partial\beta}\ . \tag{14}$$

Next, we will use these ideals to study the quantum equivalent of the BEG model.

A. Phase diagram

To obtain the phase diagram of the Hamiltonian we have to determine the critical curve as well as the tricritical point which separates the first-order transition line from the second-order one. The first step of this program can be easily performed by using the well-established properties of the phenomenological renormalization group.[9] However, to find the tricritical point some remarks are in order. First, we remember that in an extended parameter space (which includes the magnetic field H), the first-order line is characterized by coexistence of three phases: two ordered ferromagnetic ($\langle S\rangle\neq 0$) and a disordered phase ($\langle S\rangle=0$). Second, we notice that the average size of the ordered domains ($\langle S\rangle\neq 0$) is related to the quantity

$$\xi_L=[\ln(\lambda_0/\lambda_1)]^{-1},$$

while the average size of the disordered domain ($\langle S\rangle=0$) is determined by the persistence length[15]

$$\tilde{\xi}_L=[\ln(\lambda_0/\lambda_2)]^{-1},$$

where $\lambda_0,\lambda_1,\lambda_2$ are the three largest eigenvalues of the transfer matrix (T) of the model.

At the tricritical point the disordered paramagnetic and the two ordered phases becomes indistinguishable, which requires the asymptotic degeneracy of the three largest eigenvalues of T.

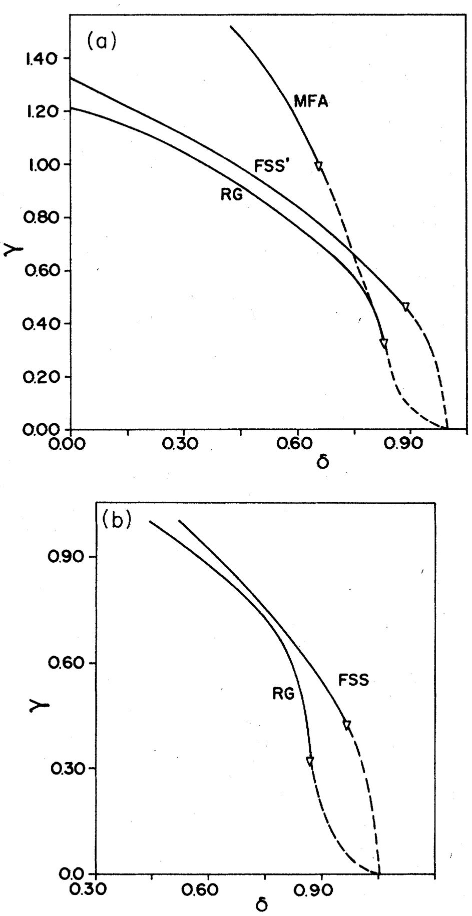

FIG. 1. Phase diagram of the Hamiltonian [Eq. (7)] for the coupling (a) $\alpha=\lambda=0$, (b) $\alpha=0$, $\lambda=0.1$. Our results (FSS) are plotted together with those obtained by mean-field approximation (MFA) and real-space renormalization-group techniques[7] (RG). The triangle (∇) locates the tricritical point separating first- (dashed) and second- (solid) order transition lines.

TABLE I. Estimates of the tricritical point in the subspace $\alpha=0$, $\lambda=0$.

Lattices	γ	δ	γ	δ
2,3	0.431 10	0.902 74	0.430 76	0.909 84
3,4	0.420 00	0.908 19	0.419 93	0.910 34
4,5	0.417 23	0.909 45	0.417 21	0.910 42
5,6	0.416 18	0.909 88	0.416 27	0.910 39
6,7	0.415 88	0.910 08	0.415 89	0.910 39
7,8	0.415 71	0.910 18	0.415 72	0.910 36
8,9	0.415 63	0.910 24	0.415 64	0.910 35

In finite systems the asymptotical degeneracy of the two largest eigenvalues is found by imposing that

$$L\xi_L^{-1}(\beta)=L'\xi_{L'}^{-1}(\beta),$$

whose counterpart in a lattice Hamiltonian field theory is

$$LG_L(\beta)=L'G_{L'}(\beta). \tag{15a}$$

If we generalize the above procedure, we locate the tricritical point by solving the equation

$$L\tilde{G}_L(t)=L'\tilde{G}_{L'}(t), \tag{15b}$$

where t parametrizes the critical curve previously obtained with Eq. (15a).

$$\tilde{G}_L=E_2-E_0$$

is the next gap which vanishes as $L\to\infty$, and t approaches the tricritical point. The phase diagrams, so obtained, are shown in Fig. 1(a) and 1(b), and our results for the tricritical point are presented in Tables I and II, for the cases $\alpha=\lambda=0$, $\alpha=0$, and $\lambda=0,1$, respectively. In the first two columns of Table I (II) we list the tricritical point estimates obtained by solving Eq. (15a) and Eq. (15b) simultaneously, whereas in the remaining columns the listed results are the crossing points between the extrapolated critical line and the solutions of Eq. (15b) for the lattice pair $(L,L+1)$. To clarify the above procedure, we have plotted both sequences of estimates for tricritical point in the $\lambda=0$ case (Fig. 2). For the sake of comparison we have included in Fig. 1 the results of a mean-field-like variational method and of a real-space renormalization-group calculation.[7] Finally, we wish to comment on the numerical part of calculations. In this analysis we have considered lattices up to $L=9$ sites (3 states per site) and evaluated the lowest eigenvalues of the

TABLE II. Estimates of the tricritical point in the subspace $\alpha=0$, $\lambda=0.1$.

Lattices	γ	δ	γ	δ
2,3	0.450 17	0.955 82	0.450 12	0.953 03
3,4	0.435 55	0.960 48	0.435 53	0.959 54
4,5	0.431 55	0.961 73	0.431 54	0.961 31
5,6	0.430 02	0.962 20	0.430 01	0.961 99
6,7	0.429 31	0.962 43	0.429 31	0.962 31
7,8	0.428 94	0.962 54	0.428 94	0.962 47
8,9	0.428 73	0.962 62	0.428 73	0.962 56

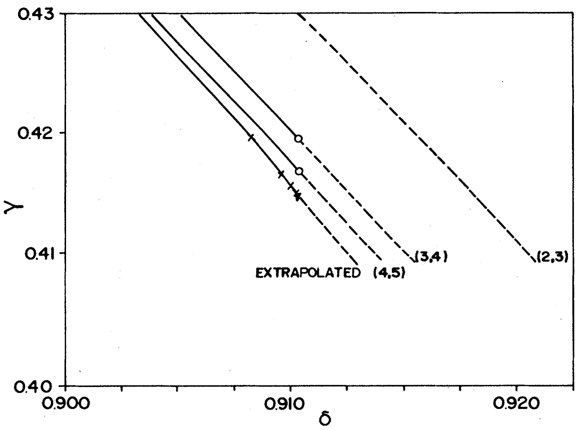

FIG. 2. Critical line estimates obtained for lattice pairs $(L, L+1)$ as well as the extrapolated curve. The tricritical points estimates represented by open circles (crosses) are the solutions of Eq. (15b) in the $(L, L+1)$ (extrapolated) curve.

Hamiltonian H using the Lanczos scheme of tridiagonalization. In order to save computer memory we represent any quantum state by an integer number whose binary code (2 bits per spin) gives its spin configuration.

B. Tricritical exponents

In this section we present two different ways, which will be henceforth named A and B, to compute the tricritical indices. Method A is a natural consequence of the special scaling of the two mass-gaps at the tricritical point, while method B essentially consists in a numerical search of the scaling directions.

1. Method A

In the neighborhood of a tricritical point we have two relevant scaling fields, ϵ and μ, which are functions of the parameters γ and δ, namely,

$$\epsilon = a(\gamma-\gamma_t)+b(\delta-\delta_t) , \tag{16a}$$

$$\mu = c(\gamma-\gamma_t)+d(\delta-\delta_t) . \tag{16b}$$

Moreover, the first and second mass gap should scale as

$$G_L(\gamma,\delta) \sim L^{-1}F(L^{y_2}\epsilon, L^{y_4}\delta) , \tag{17a}$$

and

$$\tilde{G}_L(\gamma,\delta) \sim L^{-1}\tilde{F}(L^{y_2}\epsilon, L^{Y_4}\delta) , \tag{17b}$$

where y_2, y_4 are tricritical indices associated with the scaling field ϵ and μ, respectively. The γ and δ derivatives of Eq. (17) are easily calculated, yielding

$$\frac{\partial G_L}{\partial\gamma} = aL^{-1+y_2}\frac{\partial G_L}{\partial\epsilon} + bL^{-1+y_4}\frac{\partial G_L}{\partial\mu} , \tag{18a}$$

$$\frac{\partial G_l}{\partial\delta} = cL^{-1+y_2}\frac{\partial G_L}{\partial\epsilon} + dL^{-1+y_4}\frac{\partial G_L}{\partial\mu} , \tag{18b}$$

and similar equations for $\tilde{G}$.

In order to obtain the tricritical indices, we need to eliminate directional constants by using Eq. (18) for lattices L and $L+1$, the exponents y_2 and y_4 being given by

$$y_i = 1+[\ln(\mu_i)/\ln(L/L+1)] , \quad i=2,4 , \tag{19}$$

where

$$\mu_i = [-B+(-1)^{i/2}(B^2-4AC)^{1/2}]/2A , \tag{20}$$

with

$$A = (\partial_\gamma\tilde{G}_{L+1})(\partial_\delta G_{L+1}) - (\partial_\gamma G_{L+1})(\partial_\delta\tilde{G}_{L+1}) , \tag{21}$$

$$\begin{aligned} B = {} & (\partial_\gamma G_L)(\partial_\delta\tilde{G}_{L+1}) - (\partial_\gamma\tilde{G}_L)(\partial_\delta G_{L+1}) \\ & + (\partial_\gamma G_{L+1})(\partial_\delta\tilde{G}_L) - (\partial_\gamma\tilde{G}_{L+1})(\partial_\delta G_L) , \end{aligned} \tag{22}$$

and

$$C = (\partial_\gamma\tilde{G}_L)(\partial_\delta G_L) - (\partial_\gamma G_L)(\partial_\delta\tilde{G}_L) . \tag{23}$$

This method, which has succeeded in describing tricriticality in metamagnetic models[10] and branched polymers,[16] gives, for the tricritical indices of the BEG model, the results shown in Table III. In the same table we have included the indices, obtained by extrapolating our data to $L \to \infty$.

2. Method B

A direct way to calculate the tricritical indices emerges from Eqs. (13) and (14) if we know *a priori* the relevant field ϵ and μ as functions of γ and δ. In those particular directions (parallel to ϵ or μ) our problem reduces to the usual one-relevant-field case which can be solved by a standard FSS procedure

$$G_L(\gamma,\delta) \sim L^{-1}F(L^{y_2}\epsilon, L^{y_4}\mu) \xrightarrow{\mu=0} L^{-1}F(L^{y_2}\epsilon, 0) .$$

This method consists in searching the scaling directions by requiring the invariance of the critical exponents with

TABLE III. Tricritical exponent estimates via method A.

Lattices	$\alpha=0,\ \lambda=0$ y_2	y_4	$\alpha=0,\ \lambda=0.1$ y_2	y_4
3,4	1.780 13	0.636 36	1.788 44	0.628 49
4,5	1.786 99	0.655 02	1.794 39	0.649 73
5,6	1.789 18	0.669 21	1.796 92	0.665 79
6,7	1.792 04	0.680 99	1.798 18	0.678 38
7,8	1.794 30	0.690 44	1.798 88	0.688 56
8,9	1.795 97	0.698 23	1.799 30	0.696 97
Extrapolated	1.80<u>5</u>	0.74<u>0</u>	1.80<u>1</u>	0.74<u>4</u>

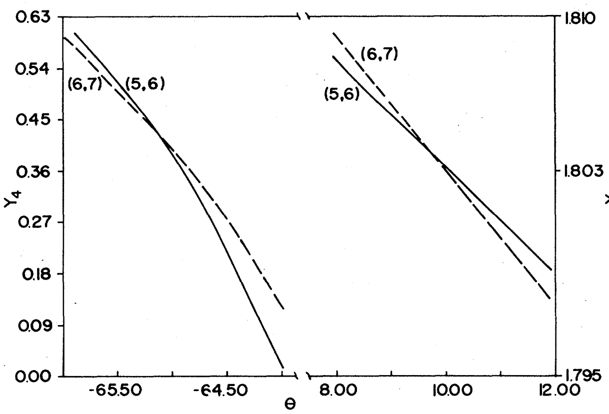

FIG. 3. The effective exponent in direction θ (measured in degrees) about the critical point. The solid (dashed) line is derived from the lattice pair 5,6 (6,7). The two crossing points are the estimators for the tricritical exponents and the angles corresponding to the scaling directions.

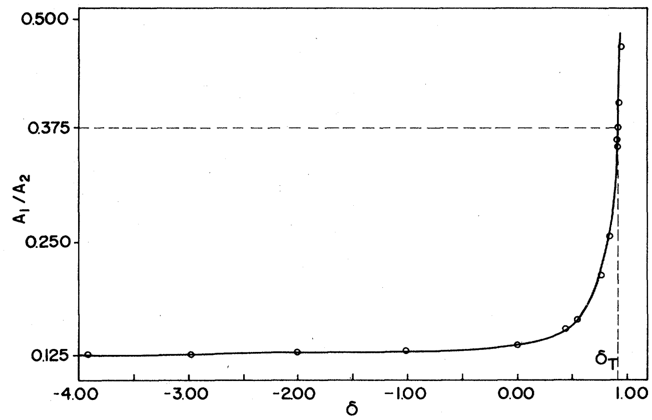

FIG. 4. Amplitude ratio A_1/A_2 at the critical line as a function of δ, in the subspace $\alpha=\lambda=0$. As $\delta\rightarrow-\infty$ the ratio approaches 0.125 which is $[\eta/2(2-1/\nu)]_{\text{Ising}}=0, 25/2(1)$. At the tricritical point the ratio tends to 0, 375 which is $[\eta/2(2-1/\nu)]_{\text{tricritical}}=0, 15/2(2-1,8)=0,375$.

the lattice size. In Fig. 3 we show the result of this procedure for the lattices $L=5,6$, and 7 while in Table IV we list the complete sequence of the results ranging from $L=2$ to $L=9$.

It is interesting to mention that one of the scaling directions is just the tangent to the critical line, at the tricritical point, while the other one makes an angle around 10° with the δ axis. Following Eq. (17b) we could also have used the second gap instead of the first one in order to search the scaling directions. Unfortunately our numerical results indicate that the second gap derivatives have bigger corrections to scaling compared with those of the first gap. Despite this, as already noted previously for a different model,[17] we find that the second gap derivative in the direction parallel to the critical line gives a reasonable estimate for the critical index

$$y_4=0.69(8) .$$

For the sake of comparison we show in Table V our results for the critical indices, together with previously existing estimates. We observe that the dominant eigenvalue obtained in this paper is in complete agreement with the conjecture of Nienhuis[18] while the subdominant one is systematically lower than the conjectured value. It is worth mentioning that the quality of the estimates for y_4 is consistently worse than for y_2, as one may reasonably expect.

IV. AMPLITUDES

In the finite-size scaling theory for an infinitely long strip ($L\times\infty$) the inverse-correlation length should vanish at $T=T_c$ as

$$\xi^{-1}\sim A/L , \tag{24}$$

where A is the so-called amplitude of correlation length. Recently an interesting conjecture concerning the universality of that amplitude has been proposed,[19] namely,

$$A=\pi\eta , \tag{25}$$

where η is the critical exponent of the two-point correlation function. Later, this conjecture was extended to include anisotropic models as well as other correlation lengths and associated exponents.[20]

In the case of a quantum Hamiltonian, as mentioned previously, the counterpart of the several correlation lengths are the various mass gaps

$$G_i=A_i/L , \tag{26}$$

and the universal quantities seem to be the ratio of the mass-gap amplitudes[21,22] A_j/A_i $j=1,2,3,\ldots$, $i=2,3,4,\ldots$) instead of the amplitude itself.

Now the relation (25) is replaced by[21–23]

$$A_i/A_j=x_i/x_j , \tag{27}$$

TABLE IV. Tricritical exponent estimates via method B.

Lattices	θ (degrees)	y_2	θ (degrees)	y_4
2,3,4	5.64	1.822 17	−64.47	0.321 70
3,4,5	7.54	1.811 55	−64.87	0.376 55
4,5,6	8.64	1.807 39	−65.10	0.418 90
5,6,7	9.77	1.804 18	−65.29	0.456 97
6,7,8	10.13	1.802 54	−65.44	0.490 89
7,8,9	10.98	1.801 82	−65.53	0.519 18
Extrapolated		1.80$\underline{1}$		0.6$\underline{4}$

TABLE V. Critical indices of the BEG model. (1D and 3D denote one-dimensional and three-dimensional, respectively.)

	y_2	y_4
Mean-field approximation[a]	2	1
RG on the classical 2D BEG model[b]	1.837	0.918
RG on the quantum 1D BEG model[c]	1.816	0.932
$\epsilon=3-d$ expansion[d]	1.968	1.2
Migdal-Kadanoff RG on the classical 2D BEG model[e]	1.773	0.516
Monte-Carlo renormalization group[f]	1.80	0.84
Finite-size scaling on the quantum 1D BEG model (this work)	1.80	0.74
Conjectured values[g]	1.80	0.80

[a]See Ref. 1.
[b]See Ref. 3.
[c]See Refs. 7 and 8.
[d]See Ref. 4.
[e]See Ref. 2.
[f]See Ref. 6.
[g]See Ref. 18.

where x_i (x_j) is the anomalous dimension of the operator related to the corresponding mass gap G_i (G_j).[24] If the mass gaps involved in Eq. (27) are the first and second ones, we get

$$A_1/A_2=x_m/x_E=(\eta/2)/(2-1/\nu) , \tag{28}$$

since the associated operators are, in this case, spin and energy density.

Using Eq. (27) we have calculated the amplitude ratios at the tricritical point, and the results (shown in Table VI) are in complete agreement with the conjectured values also presented in that table.

We have also calculated the amplitude ratio A_1/A_2 along the critical line for $\alpha=\lambda=0$ (Fig. 4). It is interesting to notice that, although we are dealing with small lattices ($L\leq 9$), we clearly see a crossover behavior separating regions belonging to different universality classes. In fact, as δ goes to $-\infty$, the ratio A_1/A_2 approaches 0.125 which is

$$\left.\frac{\eta}{2(2-1/\nu)}\right|_{\text{Ising}}=\frac{0.25}{2(2-1)}=0.125 ,$$

while at the tricritical point the ratio is approximately equal to

$$\left.\frac{\eta}{2(2-1/\nu)}\right|_{\text{tricritical}}=\frac{0.15}{2(2-1.8)}=0.375 ,$$

where we have used the value 0.15 for the index η.[25]

V. CONCLUSIONS

In this work we have analyzed the quantum version of the two-dimensional Blume-Emery-Griffiths model. We have obtained its phase diagram and located the tricritical point that separates the λ line from the first-order transition line. The tricritical exponents were calculated by two different methods, and the indices are in complete agreement with the conjecture of Nienhuis. We have also presented some results which confirm the connection between ratios of mass-gap amplitudes and critical exponents. We thus conclude that finite-size scaling ideas are very well applicable to locate tricritical points and calculate its critical indices.

ACKNOWLEDGMENT

Work supported in part by Conselho Nacional de Desenvolvimento Científico e Tecnológico (CNPq).

TABLE VI. Amplitude ratios for various lattice sizes. Using the extrapolated value of the ratio A_4/A_2 and y_2 obtained from Table III we get $y_4=0.804$, to be compared with the conjectured value $y_4=0.80$ obtained from the last line in this table [$A_4/A_2=(2-y_4)/(2-y_2)$].

Lattice	A_1/A_2	A_1/A_3	A_1/A_4	A_4/A_2
2	0.4076	0.0973	0.0864	4.7163
3	0.3949	0.0902	0.0744	5.3046
4	0.3890	0.0879	0.0070	5.5547
5	0.3857	0.0869	0.0678	5.6861
6	0.3837	0.0864	0.0665	5.7647
7	0.3823	0.0861	0.0657	5.8159
8	0.3813	0.0859	0.0651	5.8516
9	0.3807	0.0858	0.0647	5.8776
Extrapolated	0.3785	0.0856	0.0633	5.9794
Conjectured	0.3750	0.0857	0.0625	6.0000

*Present address: Department of Chemistry, University of California, San Diego, La Jolla, CA 92093.

[1]M. Blume, V. J. Emery, and R. B. Griffiths, Phys. Rev. A **4**, 1071 (1971).

[2]M. Kaufman, R. B. Griffiths, J. M. Yeomans, and M. E. Fisher, Phys. Rev. B **23**, 3448 (1981).

[3]A. N. Berker and M. Mortis, Phys. Rev. B **14**, 4969; see also T. W. Burkhardth, *ibid.* **14**, 1196 (1976).

[4]T. S. Chang, G. F. Tuthill, and H. E. Stanley, Phys. Rev. B **9**, 4882 (1974).

[5]J. M. Yeomans and M. E. Fisher, Phys. Rev. B **24**, 2825 (1981); see also Ref. 2

[6]D. P. Landau and R. Swendsen, Phys. Rev. Lett. **46**, 1937 (1981).

[7]H. Hamber, Phys. Rev. B **21**, 3999 (1980); Y. Gefen, Y. Imry, and D. Mukamel, *ibid.* **23**, 6099 (1981); D. Boyanovsky and L. Masperi, Phys. Rev. D **21**, 1550 (1980).

[8]B. Hu, Phys. Rev. Lett. **75A**, 372 (1980).

[9]M. P. Nightingale, Physica **83A**, 561 (1976).

[10]P. A. Rikvold, W. Kinzel, J. D. Gunton, and K. Kaski, Phys. Rev. B **28**, 2686 (1983); see also H. J. Herrmann, Phys. Lett. **100A**, 256 (1984).

[11]M. E. Fisher and A. E. Ferdinand, Phys. Rev. Lett. **19**, 169 (1967); A. E. Ferdinand and M. E. Fisher, Phys. Rev. **185**, 832 (1969); M. E. Fisher and M. N. Barber, Phys. Rev. Lett. **28**, 1516 (1972); *Critical Phenomena, Proceedings of the International School of Physics "Enrico Fermi" Course 51, Varenna, 1970,* edited by M. S. Green (Academic, New York, 1971).

[12]The phenomenological renormalization-group approximation was put on firmer ground by E. Brezín, J. Phys. (Paris) **43**, 15 (1982).

[13]For a detailed description of the method we refer to the review paper of M. N. Barber, in *Phase Transitions and Critical Phenomena,* edited by C. Comb and J. L. Lebowitz (Academic, London, 1983), Vol. 8.

[14]The condition (10) can also be used to locate first-order transition points accurately as shown in previous calculations [P. A. Rikvold, K. Kaski, J. D. Gunton and M. C. Yalabik, Phys. Rev. B **29**, 6285 (1984) and Ref. 10]. For a detailed discussion see V. Privmann and M. E. Fisher, J. Stat. Phys. **33**, 385 (1983).

[15]M. E. Fisher and A. N. Berker, Phys. Rev. **26**, 2507 (1982).

[16]B. Derrida and H. J. Hermann, J. Phys. (Paris) **44**, 1365 (1983).

[17]P. de Beale, J. Phys. A **17**, 1335 (1984).

[18]B. Nienhuis, J. Phys. A **15**, 199 (1982).

[19]J. M. Luck, J. Phys. A **15**, L169 (1982); B. Derrida and L. de Seze, J. Phys. (Paris) **43**, 475 (1982); see also, J. Cardy, J. Phys. A **17**, L385 (1984).

[20]H. Blöte and M. P. Nightingale, J. Phys. A **16**, L657 (1983).

[21]K. A. Penson and M. Kolb, Phys. Rev. B **30**, 470 (1984).

[22]F. C. Alcaraz and J. R. Drugowich de Felício, J. Phys. A **17**, L651 (1984).

[23]G. V. Gehlen, C. Hoeger, and V. Rittenberg, J. Phys. A **17**, L469 (1984).

[24]In a previous paper (see Ref. 22) two of us have obtained for the Ashkin-Teller model a relation between critical indices and the amplitude itself.

[25]R. B. Pearson, Phys. Rev. B **22**, 2579 (1980); B. Nienhuis, E. K. Riedel, and M. Schick, J. Phys. A **13**, L31 (1980); **13**, L189 (1980).